and a solution of *n*-butyllithium (1.13 mL, 1.6 M in hexane, 1.8 mmol) was added dropwise (exothermic reaction). After stirring for 1 h at −74 °C, the mixture was transferred via cannula to a solution of (*R*,*R*)-**15** (1.225 g, 2.0 mmol) in 50 mL of ether, precooled to −74 °C. Stirring at −74 °C was continued for 2.5 h, and benzaldehyde (**3**, 0.16 g, 1.6 mmol) was added to the dark brown solution of (*R*,*R*)-**51**. After stirring for 3 h at −74 °C, the reaction was worked up as usual. Chromatography (80 g of silica gel, hexane/ether/CH_2Cl_2 5:1:1) afforded 0.24 g (68%) of (*R*)-**61** ($[\alpha]_D$ = −46.43 (*c* = 2.8, $CHCl_3$)), ≥95% ee, according to GLC analysis (carrier 50 kPa, 140 °C, derivatization with *N*-isopropyl isocyanate): (1*R*,2*S*) isomer, (*R*)-**61** t_R = 19.3 min; (1*S*,2*R*) isomer, (*S*)-**61** t_R = 19.6 min (obtained with (*R*)-**61** in a reaction using $Cp(2\text{-}PrO)_2TiCl$ **42** for transmetalation, not detected); ≥95% de as the (1*RS*,2*RS*) diastereomer (syn) was not detected by ^1H and ^{13}C NMR; ^1H NMR ($CDCl_3$, 400 MHz) 7.23-7.35 (m, C_6H_6), 5.86 (ddd, *J* = 17.0, 10.0, 10.0, H-C(3)), 5.11 (dd, *J* = 10.0, 2.0, H-C(4)), 5.02 (dd, *J* = 17.0, 2.0, H-C(4)), 4.79 (dd, *J* = 8.5, 2.0, H-C(1)), 2.20 (d, *J* = 2.0, OH), 2.08 (dd, *J* = 10.0, 8.5, H-C(2)), −0.21 (s, $Si(CH_3)_3$); ^1H NMR (CCl_4, 250 MHz) 7.23-7.35 (m, C_6H_6), 5.73 (ddd, *J* = 17.0, 10.5, 10.5, H-C(3)), 4.87 (dd, *J* = 10.5, 2.0, H-C(4)), 4.73 (dd, *J* = 17.0, 2.0, H-C(4)), 4.70 (dd, *J* = 6.5, 2.0, H-C(1)), 1.64 (d, *J* = 2.0, OH), 1.90 (dd, *J* = 10.5, 6.5, H-C(2)), −0.21 (s, $Si(CH_3)_3$).

36. (3*S*,4*R*)-3-(Trimethylsilyl)-1-tridecen-4-ol ((*R*)-62). Reaction of decanal (285 mg, 1.825 mmol) with (*R*,*R*)-**51** as described above for benzaldehyde (**3** → **61**) afforded 0.34 g (69%) of (*R*)-**62**, purified by chromatography (80 g of silica gel, hexane/ether/CH_2Cl_2 5:1, $[\alpha]_D$ = 1.40 (*c* = 3.5, $CHCl_3$)), ≥95% ee, as determined by ^1H NMR (addition of (*S*)-2,2,2-trifluoro-1-(9′-anthryl)ethanol (TFAE)[51]): (3*S*,4*R*) isomer, (*R*)-**62** δ H_{cis}-C(1) = 4.94; (3*R*,4*S*) isomer, (*S*)-**62** δ H_{cis}-C(1) = 4.91 ppm (not observed, racemic **62** was produced using $Cp(2\text{-}PrO)_2TiCl$ **42** for transmetalation); ^1H NMR ($CDCl_3$, 400 MHz) 5.80 (ddd, *J* = 17.0, 10.5, 10.5, H-C(2)), 5.04 (dd, *J* = 10.5, 2.5, H-C(1)), 4.93 (dd, *J* = 17.0, 2.0, H-C(1)), 3.79 (m, H-C(4)), 1.68 (dd, *J* = 10.5, 5.5, H-C(3)), 1.46 (d, *J* = 4.5, OH), 1.34-1.21 (m, 16 H), 0.83 (t, *J* = 6.75, CH_3), 0.04 (s, $Si(CH_3)_3$).

Supplementary Material Available: Tables of crystal structure data, positional parameters, displacement parameters, bond distances, and bond angles (8 pages); tables of observed and calculated structure factors (28 pages). Ordering information is given on any current masthead page.

Gas-Phase Electron-Transfer Reactions between Selected Molecular Anions and Halogenated Methanes

W. B. Knighton and E. P. Grimsrud*

Contribution from the Department of Chemistry, Montana State University, Bozeman, Montana 59717. *Received March 25, 1991. Revised Manuscript Received July 11, 1991*

Abstract: The products and rate constants for the thermal gas-phase reactions of eight halogenated methanes (RX), including CCl_4, $CFCl_3$, CF_2Cl_2, $CHCl_3$, CH_3I, CCl_3Br, CF_2Br_2, and CH_2Br_2, with selected molecular anions (A^-), including azulene(−), nitrobenzene(−), and several substituted nitrobenzenes(−), are reported. The electron affinities of the donor molecules (A) range from 16 kcal mol^{-1} for azulene to 46 kcal mol^{-1} for *p*-dinitrobenzene. CCl_4, CCl_3Br, and CF_2Br_2 react rapidly with several A^- to form halide ions (X^-) and clustered halide ions ($A{\cdot}X^-$). No molecular ions of the type RX^- are observed as reaction products. For these three halomethanes, a continuous decrease in the reaction rate constants with increased electron affinity of A is observed. The other five halomethanes react either with none of the molecular anions or only with Az^-. The products and rates of these reactions are shown to be consistent with an electron-transfer mechanism in which the clustered halide ion, $A{\cdot}X^-$, rather than X^-, is first formed in a two-part reaction sequence. The low reactivities of $CFCl_3$, CF_2Cl_2, $CHCl_3$, CH_3I, and CH_2Br_2 with the molecular anions can be explained in terms of unfavorable polarizabilities and unfavorable dipole-moment-induced orientations for these molecules in the transition states of the proposed mechanism.

Introduction

Several classes of compounds have been shown to react rapidly with either thermal electrons or electron donors to form stable negative ions in the gas phase. In these studies, a diversity of mechanistic behaviors for electron-capture (EC) and electron-transfer (ET) processes have been revealed.[1-5] For EC reactions,[1] several classes of compounds (nitroaromatics and perfluorinated alkanes, for example) have been shown to undergo EC by the resonance electron capture (REC) mechanism, shown as reaction 1 in which an excited intermediate, A^{-*}, has a sufficiently long

$$e + A \rightleftharpoons A^{-*} \rightarrow A^- \qquad (1)$$

lifetime that it is collisionally stabilized in a bath gas of moderately high pressure. Several other classes of compounds (chlorinated, brominated, and iodinated alkanes, for example) have been found to undergo thermal EC by the dissociative electron capture (DEC) mechanism, reaction 2, in which an excited intermediate, RX^{-*},

$$e + RX \rightarrow RX^{-*} \rightarrow R + X^- \qquad (2)$$

has a very short lifetime against dissociation relative to the time required for stabilizing collisions with a bath gas. Even though some halogenated alkane molecules, RX, are known to have positive electron affinities (EA), molecular anions, RX^-, have never been observed as stable reaction products in their EC reactions.

The formation of molecular anions A^- by resonance electron transfer (RET) from donor molecular anions B^-, as shown in reaction 3, have been extensively studied[2,3,5] for compounds A and

$$B^- + A \rightleftharpoons B + A^- \qquad (3)$$

B of the type that tend to form stable molecular anions upon exposure to thermal electrons by REC (reaction 1). It has been noted that most RET reactions (those of substituted aromatic compounds, substituted benzo-, naphtho-, and anthroquinones, and tetracyanoethylene, for example) occur at near collision frequency as long as the reaction is exothermic by a few kilocalories

(1) Wentworth, W. E.; Chen, E. C. M. In *Electron Capture, Theory and Practice in Chromatography*; Zlatkis, A., Poole, C. F., Eds.: Elsevier Scientific Publishing Co.: New York, 1981; pp 27-68.
(2) Fukuda, E. K.; McIver, R. T. *J. Chem. Phys.* **1982**, *77*, 4942.
(3) Grimsrud, E. P.; Caldwell, G.; Chowdhury, S.; Kebarle, P. *J. Am. Chem. Soc.* **1985**, *107*, 4627.
(4) Grimsrud, E. P.; Chowdhury, S.; Kebarle, P. *J. Chem. Phys.* **1985**, *83*, 1059.
(5) Kebarle, P.; Chowdhury, S. *Chem. Rev.* **1987**, *87*, 513.

0002-7863/92/1514-2336$03.00/0

per mole or more. An exception to this general trend was noted, however, in the RET reactions of perfluorinated compounds, including SF_6 and C_7F_{14}, where low reaction efficiencies were observed even for reaction systems of moderate exothermicity, up to 20 kcal mol^{-1}.[4]

Considering the fundamental importance of electron-transfer processes, it its noteworthy that little attention has been given, to date, to the nature of electron-transfer reactions between molecular anions of the type A^-, which are formed by the REC mechanism (reaction 1), and neutral compounds of the type RX, which react with thermalized electrons by the DEC mechanism (reaction 2). It is therefore unknown which, if any, of the following mechanisms might be operative in such reactions.

$$A^- + RX \longrightarrow \begin{cases} A + R + X^- & (4a) \\ A + RX^{-*} & (4b) \end{cases}$$

$$A^- + RX \rightarrow AR + X^- \quad (5)$$

Reaction 4a is a dissociative electron transfer (DET) and would be possible if the difference in EA of compounds RX and A exceeds the R–X bond energy in the intermediate species RX^{-*}. Reaction 4b is a simple RET (reaction 3) and might be expected if the EA difference between RX and A is less than the R–X bond energy in RX^{-*}. The occurrence of reaction 4b would be particularly significant, because it would lead to the rarely observed molecular anions RX^- of the halogenated methanes. Alternatively, the S_N2 nucleophilic displacement mechanism, shown as reaction 5, might be operative. In this reaction, the formation of an A–R bond in the neutral product would provide an additional thermochemical driving force for the production of X^-.

Previous investigations of reactions between molecular anions and DEC-active halogenated methanes include the following studies in which relatively small molecular anions were used in each case. Rinden et al.[6] reported that NO^- reacts with CCl_4 and CH_3I to form Cl^- and I^-, respectively. Since the EA of NO is very low (0.5 kcal mol^{-1}), the internal energy imparted to an intermediate, RX^{-*}, by the DET mechanism (reaction 4a) would be almost equal to that imparted to the corresponding DEC intermediate in reaction 2. Therefore, the reactions of NO^- with CCl_4 and CH_3I might have occurred by the DET mechanism (reaction 4a). The S_N2 mechanism (reaction 5) would be even more exothermic, however, and NO^- is a viable S_N2 nucleophile in that it is small and capable of bonding to a carbon-centered substrate. For these reasons, Rinden et al. could not conclude whether these reactions occurred by the DET or the S_N2 mechanism. Fehsenfeld et al.[7] reported that O_2^- reacts rapidly with CF_2Cl_2 and $CFCl_3$ to form almost entirely Cl^- along with very small amounts of the molecular anions $CF_2Cl_2^-$ and $CFCl_3^-$. Because the EA of O_2 is relatively low (10 kcal mol^{-1}), the production of Cl^- was again thermochemically consistent with either the DET or S_N2 mechanisms. The observation of molecular anions $CF_2Cl_2^-$ and $CFCl_3^-$ suggested that the RET mechanism (reaction 4b) was at least minimally operative in these reaction systems. Dispert and Lacmann[8] have also reported low but measurable yields of molecular anions along with the major ion Cl^- by collisions of CCl_4, $CFCl_3$, and CF_2Cl_2 with neutral potassium atoms in a molecular beam of controlled kinetic energy. The appearance potentials for the molecular anions observed in that study indicated EA values of 46 ± 5, 24 ± 7, and 9 ± 7 kcal mol^{-1} for CCl_4, $CFCl_3$, and CF_2Cl_2, respectively.

In the present study, the ion–molecule reactions between a set of molecular anions, including azulene(–), nitrobenzene(–), and several substituted nitrobenzenes(–), and a set of halogenated methanes, including CCl_4, $CFCl_3$, CF_2Cl_2, $CHCl_3$, CCl_3Br, CF_2Br_2, CH_2Br_2, and CH_3I, have been investigated. The electron affinities of the electron donors used in this study are well known[5] and allow systematic variation of electron donor energy over a range of 30 kcal mol^{-1}. All of the halogenated methanes studied here are known to capture thermal electrons rapidly by the DEC mechanism. Measurements of the rates and the products of the ion–molecule reactions have been made by a pulsed e-beam high-pressure mass spectrometer (PHPMS) at a pressure of 3 Torr and 125 °C. The temperature dependencies and activation energies for four reaction systems are also reported.

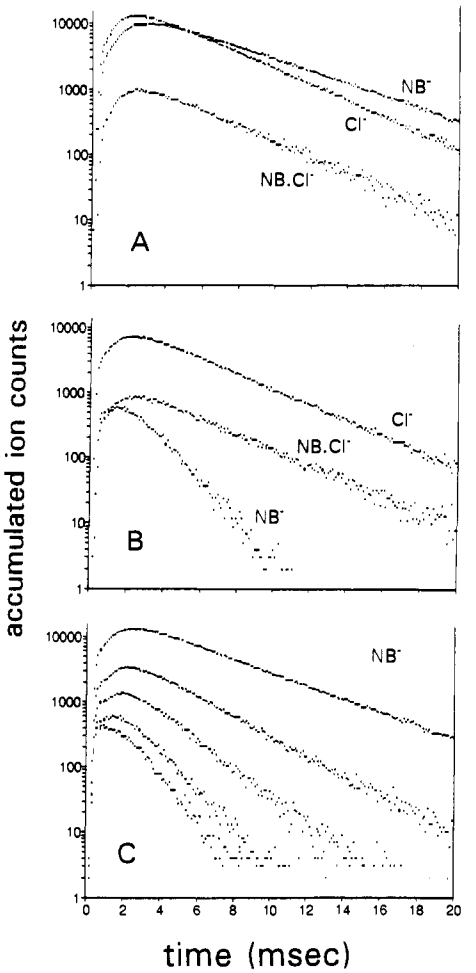

Figure 1. Pulsed e-beam high-pressure mass spectrometry measurements of the molecular ion of nitrobenzene, the chloride ion, and the nitrobenzene–chloride cluster ion at 125 °C in 3.0 Torr of methane buffer gas that also contains (A) 1.30 mTorr of nitrobenzene with 0.091 mTorr of $CFCl_3$, (B) 1.5 mTorr of nitrobenzene with 0.100 mTorr of CCl_4, and (C) 1.50 mTorr of nitrobenzene with 0.00, 0.033, 0.067, 0.100, and 1.36 mTorr of CCl_4.

Experimental Section

The PHPMS has recently been described in detail.[9] A mixture of gas consisting of small quantities of compounds A and RX in the major diluent gas methane is first prepared in an associated gas handling plant. This mixture then flows slowly through the thermostated ion source of the PHPMS. A short pulse (20 μs) of 3000-V electrons produces positive ions and electrons within the ion source. In the 3 Torr of methane buffer gas, the secondary electrons are rapidly thermalized and then are captured by both compounds A and RX. These EC reactions produce an initial population of A^- and X^- ions (by reactions 1 and 2) which are also rapidly thermalized through collisions with the buffer gas. The A^- ions then engage in reaction with the RX neutral molecules, if such reaction is favorable. The number density of ions within the source is sufficiently low such that the dominant loss of charge is due to diffusion to the wall. The ion intensities are determined by measuring the wall current, that is, by bleeding the gas mixture through a narrow slit into an evacuated

(6) Rinden, E.; Marlcq, M. M.; Grabowski, J. J. *J. Am. Chem. Soc.* **1989**, *111*, 1203.

(7) Fehsenfeld, F. C.; Crutzen, P. J.; Schmeltekopf, A. L.; Howard, C. J.; Albritton, D. L.; Ferguson, E. E.; Davidson, J. A.; Schiff, H. I. *J. Geophys. Res.* **1976**, *81*, 4454.

(8) Dispert, H.; Lacmann, K. *Int. J. Mass Spectrom. Ion Phys.* **1978**, *28*, 49.

(9) Knighton, W. B.; Zook, D. R.; Grimsrud, E. P. *J. Am. Soc. Mass Spectrom.* **1990**, *1*, 372.

region where the ions are mass analyzed (quadrupole mass filter), detected (ion-counting channeltron), and time analyzed (multichannel scaler).

Results

The results obtained in three typical experiments are shown in Figure 1. In Figure 1A, a nonreactive system involving NB and $CFCl_3$ is shown. For a short period immediately after the e-beam pulse, all negative ion signals are weak due to a positive ion space-charge field which inhibits the diffusion of negative ions to the walls of the ion source.[3,10] As the electrons are converted to negative ions by EC reactions, the space-charge field is destroyed and negative ions begin to diffuse to the walls and are detected by the mass spectrometer. In Figure 1A, EC by NB (reaction 1) and $CFCl_3$ (reaction 2) has resulted in the formation of NB^- and Cl^- ions. For this system, no further chemical reactions occur and the loss of these two EC products is then determined only by their rates of diffusion to the walls. The diffusional loss rates for NB^- and Cl^- in Figure 1A are similar because they are determined by the reduced masses of each ion and the relatively light buffer gas CH_4.[10]

Also shown in Figure 1A is the cluster ion $NB{\cdot}Cl^-$. In this case, the cluster ion is formed from the Cl^- ion by the fast clustering equilibrium process shown as reaction 6. The intensity ratio of

$$NB + Cl^- \rightleftharpoons NB{\cdot}Cl^- \quad (6)$$

the Cl^- and $NB{\cdot}Cl^-$ ions observed in Figure 1A is held constant throughout the period of measurement because reaction 6 is fast in both directions. From previous measurements of this reaction,[11] an equilibrium constant, K_6, of 4.0×10^5 atm^{-1} and an abundance ratio for $Cl^-/NB{\cdot}Cl^-$ of 11.5 are predicted under the experimental conditions of Figure 1A. The observed intensity ratio of 12.8 is in excellent agreement with this prediction.

In Figure 1B, measurements of a chemically reactive system involving NB^- and CCl_4 are shown. In this case, NB^- and Cl^- ions are again initially formed by EC reactions. However, after about 3 ms the intensity of the NB^- ion decreases much more rapidly than in Figure 1A. This increased loss of NB^- is due to the reaction

$$NB^- + CCl_4 \rightarrow \text{products} \quad (7)$$

The only other negative ions observed for this system are Cl^- and the cluster ion $NB{\cdot}Cl^-$. While a major portion of these ions were produced by an initial EC reaction 2, it is apparent that the ionic products of the reaction between NB^- and CCl_4 must be either Cl^- or $NB{\cdot}Cl^-$. The constant relative intensity of the Cl^- and $NB{\cdot}Cl^-$ ions in Figure 1B again indicates that these two ions are coupled by the fast reaction 6.

The ions which were found to be potential products of reaction 7 are also indicated in Table I. For all cases, the major product ion observed was of the type X^-. The second most intense product ion was of the type $A{\cdot}X^-$. Since these two ions are coupled by fast equilibrium (reaction 6), it was impossible to experimentally determine which of these two ion types was the first-formed product of the reactions. It is significant to note that special attempts were made in these studies to detect molecular anions of the type RX^-. No ions of this type were ever observed, however, and their contribution to the total negative ion products of these reactions is estimated to be less than 0.01%.

The second-order rate constants for the reactions of A^- with RX were obtained by experiments such as shown in Figure 1C, where the time dependence of the NB^- signal in five separate experiments involving increasingly greater CCl_4 concentrations is shown. As expected, the rate of decrease in NB^- is proportional to the concentration of CCl_4. The slopes of the decay lines in Figure 1C provide the decay rates, v_{obs}, which have been plotted in Figure 2 against the concentration of CCl_4. A straight line

Table I. Products, Rate Constants, and Activation Energies for Reactions between Selected Molecular Anions (A^-) and Halogenated Methanes (RX)

A^-[a]	RX	major product[b]	k_7[c]	k(ADO)[d]	$\Delta E^{\pm}$[e]
Az^-	CCl_4	Cl^-	5.0	9.4	
NB^-	CCl_4	Cl^-	1.8	9.6	+3.7
o-FNB^-	CCl_4	Cl^-	0.83	9.2	
m-FNB^-	CCl_4	Cl^-	0.05	9.2	+6.8
m-CF_3NB^-	CCl_4		nd	8.5	
Az^-	$CFCl_3$	Cl^-	0.23	9.4	
NB^-	$CFCl_3$		nd	9.6	
Az^-	CF_2Cl_2		nd	9.8	
Az^-	$CHCl_3$	Cl^-	<0.01	10.4	
Az^-	CH_3I		nd	10.3	
Az^-	CCl_3Br	Br^-	14.0	9.6	
NB^-	CCl_3Br	Br^-	9.2	9.7	0.0
o-FNB^-	CCl_3Br	Br^-	8.5	9.3	
m-FNB^-	CCl_3Br	Br^-	5.9	9.3	
m-CF_3NB^-	CCl_3Br	Br^-	3.0	8.6	
o-NO_2NB^-	CCl_3Br	Br^-	0.47	8.9	+2.5
p-NO_2NB^-	CCl_3Br		nd	8.9	
Az^-	CF_2Br_2	Br^-	8.2	8.3	
NB^-	CF_2Br_2	Br^-	4.0	8.4	
o-FNB^-	CF_2Br_2	Br^-	3.2	8.1	
m-FNB^-	CF_2Br_2	Br^-	0.47	8.1	
m-CF_3NB^-	CF_2Br_2		nd		
Az^-	CH_2Br_2	Br^-	0.07	10.3	
NB^-	CH_2Br_2		nd		

[a] Az = azulene, NB = nitrobenzene. [b] The second most abundant product ion was of the type $A{\cdot}X^-$ where X^- is the halide ion indicated. [c] (cm^3 $molecule^{-1}$ s^{-1}) $\times 10^{10}$. Temperature is 125 °C. [d] (cm^3 $molecule^{-1}$ s^{-1}) $\times 10^{10}$. The following dipole moments (D) and polarizabilities (Å^3) were used: CCl_4, 0, 11.2; $CFCl_3$, 0.45, 9.5; CF_2Cl_2, 0.51, 7.8; $CHCl_3$, 1.01, 9.5; CH_3I, 1.62, 8.0; CCl_3Br, 0.2, 12; CF_2Br_2, 0.66, 9.0; CH_2Br_2, 1.43, 9.3. [e] kcal mol^{-1}.

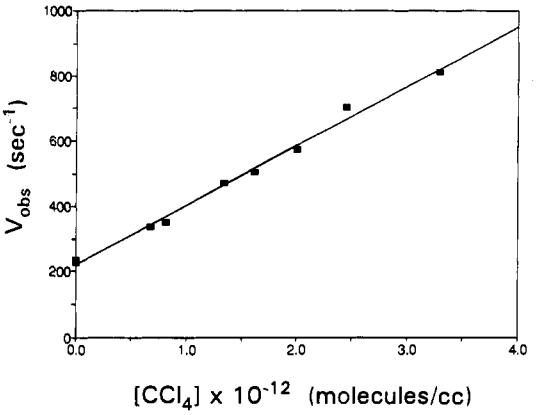

Figure 2. Observed decay rates of the NB^- ion as a function of CCl_4 concentration in experiments such as shown in Figure 1C.

is obtained in accordance with the expectation that $v_{obs} = k_7[RX] + v_d$. The slope of this line provides k_7, and the intercept, v_d, is equal to the diffusional loss rate. Rate constants, k_7, greater than about 1×10^{-12} cm^3 s^{-1} could be reliably measured by this method, and these are provided in Table I.

The reactions of each halomethane are listed in Table I in order of increasing EA of the donor molecule A, and measurements are provided for reactions up to the case where the EA of the donor is too great to allow detectable reaction. The EA values (kcal mol^{-1}) of the donors are Az, 15.9; NB, 23.3; o-FNB, 24.7; m-FNB, 28.4; m-CF_3NB, 32.5; o-NO_2NB, 38.0; and p-NO_2NB, 46.1.[5] Only CCl_4, CCl_3Br, and CF_2Br_2 were found to react with several of the electron donors. The calculated ADO rate constants[12] for the collisions of these three halocarbons with all of the molecular anions used in these studies are all about 9×10^{-10} cm^3 s^{-1}. Therefore, it is seen that the reactions of Az^- with these three

(10) Kebarle, P. In *Techniques for the Study of Ion Molecule Reactions*; Farrar, J. M., Saunders, W., Eds.; John Wiley and Sons, Inc.: New York, 1988; pp 221–286.
(11) Chowdhury, S.; Kebarle, P. *J. Chem. Phys.* **1986**, *85*, 4989.
(12) Su, T.; Bowers, M. T. In *Gas Phase Ion Chemistry*; Bowers, M. T., Ed.; Academic Press: New York, 1979.

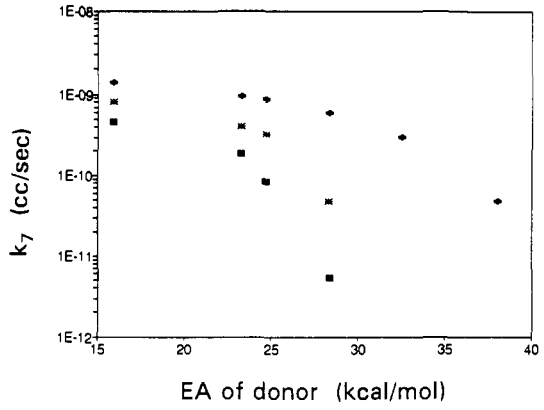

Figure 3. Observed second-order rate constants for the reactions of CCl_4 (■), CF_2Br_2 (*), and CCl_3Br (+) with a variety of molecular anions, A^-, as a function of the electron affinities of A. Temperature is 125 °C.

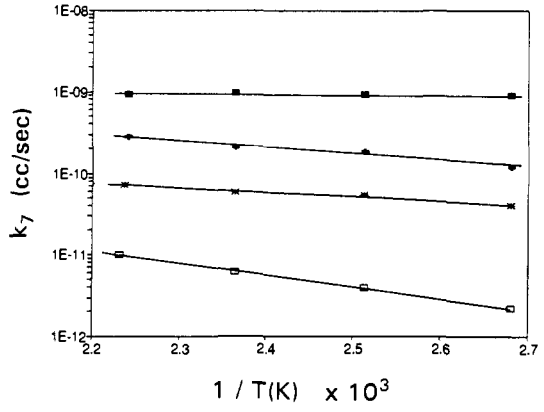

Figure 4. Temperature dependence of the rate constants for the reactions of NB^- with CCl_3Br (■), NB^- with CCl_4 (+), o-NO_2NB^- with CCl_3Br (*), and m-FNB^- with CCl_4 (□).

halocarbons occur with very high efficiency (>50%). In Figure 3, the rate constants for the reactions of CCl_4, CCl_3Br, and CF_2Br_2 have been plotted against the known EA values of the donor molecules. A continuous decrease in the rate constants with increased EA of the donor is clearly indicated for each of these three halomethanes.

For $CFCl_3$, CH_2Br_2, and $CHCl_3$, reaction was detected only with use of the lowest EA electron donor Az^-. For $CHCl_3$, this reaction was too slow for k_7 to be accurately determined. For $CFCl_3$ and CH_2Br_2, k_7 was approximately 100 times lower than k(ADO). For CF_2Cl_2 and CH_3I, no reactions with any of the electron donors, including Az^-, were observed.

The rate constants for four reaction systems were also measured over a temperature range from 100 to 180 °C, and an Arrhenius plot of these results is shown in Figure 4. Except for the collision-limited reaction of NB^- with CCl_3Br, all of the slower reactions exhibit a positive temperature dependence that is characteristic of reactions involving transition states of energy greater than that of the reagents.[13] The slopes of the best-fit straight lines drawn in Figure 4 indicate activation energies of +2.5 kcal mol$^-$ for the reaction of o-DNB^- with CCl_3Br, +3.7 kcal mol^{-1} for NB^- with CCl_4, and +6.8 kcal mol^{-1} for mFNB$^-$ with CCl_4.

Discussion

In the following discussions, it will be useful to refer to the energy level diagrams shown in Figure 5. In this figure the enthalpies of various negative ionization processes associated with the molecules studied here are indicated. In the left column the donor molecular anions are positioned (top to bottom) in accordance with their increasing enthalpies of negative ionization.

(13) Olmstead, W. N.; Brauman, J. I. *J. Am. Chem. Soc.* **1977**, *99*, 4219.

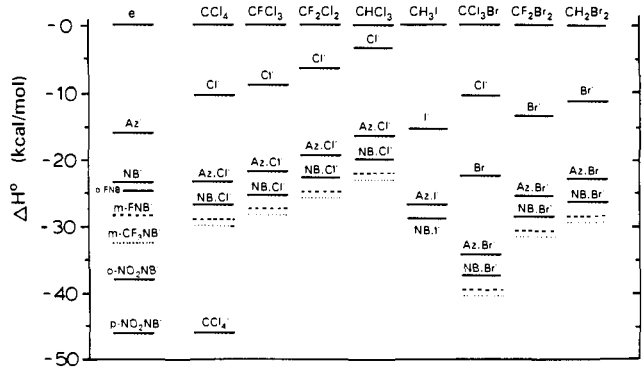

Figure 5. Energy level diagram for various negative ionization processes of the donor molecules and the halogenated methanes studied here (see text for full explanation).

Table II. Binding Energies in $A{\cdot}X^-$ from Enthalpies of Equilibrium Reactions $A + X^- \rightleftharpoons A{\cdot}X^-$

A	X^-	$-\Delta H°$ [a]	$-\Delta H°$ [b]
Az	Cl^-		13.0
NB	Cl^-	16.3	16.3
m-FNB	Cl^-	18.7	
m-CF_3NB	Cl^-	19.5	
Az	Br^-		12.0
NB	Br^-		15.1
m-FNB	Br^-		17.2
m-CF_3NB	Br^-		17.7
Az	I^-		10.6
NB	I^-		13.4
CCl_4	NB^-		<11

[a] From reference 11. Units are kcal mol^{-1}. [b] From measurements of $\Delta G°$ in the present study at various temperatures between 35 and 125 °C with the assumptions $\Delta G° = \Delta H° - T\Delta S°$ and $\Delta S° = 20$ cal K^{-1} mol^{-1}.[11] Units are kcal mol^{-1}.

The reference zero energy level at the top of this column corresponds to the energy of the free thermalized electron, while the lower (more negative) electron donor energies of the A^- species are determined by the known EA[5] of the molecules A. The other eight columns provide the enthalpy changes associated with various negative ionization processes of the halomethanes. In each of these columns, the enthalpy for the DEC process $e + RX \rightarrow R + X^-$, is indicated by "$X^-$" and has been calculated from the relation $\Delta H°_2 = +\Delta H°_f(R) + \Delta H°_f(X) - \Delta H°_f(RX) - EA(X)$, using thermochemical data provided by Lias et al.[14] The other entries in each column, indicated by "$A{\cdot}X^-$", provide the additional enthalpies which would be provided to the DEC process if the cluster ion $A{\cdot}X^-$, rather than X^-, were formed as the reaction product. The magnitude of this additional energy is equal to that of the clustering reactions $X^- + A \rightarrow A{\cdot}X^-$, which are provided for several systems in Table II. The enthalpies for four systems of the type $A{\cdot}X^-$ are provided in Figure 5 for A = Az, NB, m-FNB (dashed line), and m-CF_3NB (dotted line). The enthalpy for formation of CCl_4^- from CCl_4 reported by Dispert and Lacmann[8] is also indicated in Figure 5. By use of Figure 5, the enthalpy change for various reactions of potential interest are conveniently provided. For example, for the DET reaction $NB^- + CCl_4 \rightarrow NB + CCl_3 + Cl^-$, $\Delta H°_{4a} = +13$ kcal mol^{-1} is conveniently obtained from the difference in Figure 5 in the energy levels assigned to NB^- in the first column and Cl^- in the second.

Some General Observations. The fact that no ions of the type RX^- were observed as products in any of the reactions studied here is taken to indicate that the RET process (reaction 4b) is not important for any of these systems. In view of the relatively high EA values previously reported[8] for CCl_4 (46 ± 5 kcal mol^{-1}) and $CFCl_3$ (24 ± 7 kcal mol^{-1}), this result is somewhat surprising for at least the reactions involving these two compounds. For example, if $EA(CCl_4)$ is equal to 46 kcal mol^{-1}, inspection of

(14) Lias, S. G.; Bartmess, J. E.; Liebman, J. F.; Holmes, J. L.; Levin, R. D.; Mallard, W. G. *J. Phys. Chem. Ref. Data* **1988**, *17*, 1.

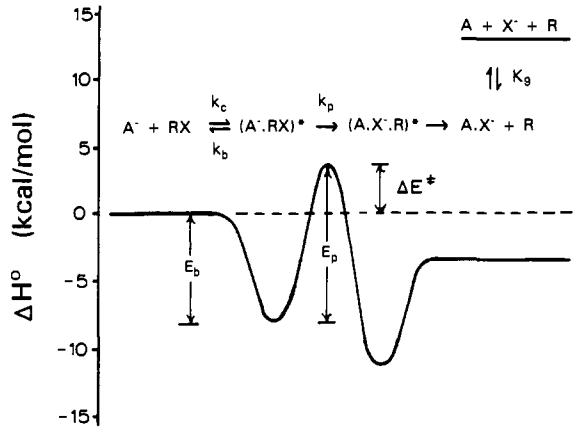

Figure 6. Proposed reaction coordinate for the CADET reactions of molecular anions (A^-) with halogenated methanes (RX). The coordinate includes two energy wells for two reaction intermediates which are separated by a high-energy transition state. The initial product formed is a halide ion that is clustered by the donor molecule ($A{\cdot}X^-$). Reequilibration of this species with the ion source gas results in the production of the halide ion (X^-) by a second equilibrium reaction (K_9). The relative energies indicated for the reagents, the two sets of products, and the transition state are those of the A = NB and RX = CCl_4 reaction system. The well depths assigned to the two intermediates have been estimated.

Figure 5 indicates that the RET reactions $A^- + CCl_4 \rightarrow A + CCl_4^-$ would have been thermochemically favorable for almost all of the electron donors studied here. Our results indicate that RET reactions of CCl_4 having low exothermicity (such as for A^- = o-DNB^-) are much too slow to be detected and those of moderate exothermicity (such as for A = Az) are overwhelmed by another, much faster reaction channel that leads to either the Cl^- or $A{\cdot}Cl^-$ ions. As was observed in a previous study[4] of the RET reactions of SF_6, the RET reactions of CCl_4 appear to be characterized by a large internal energy barrier which effectively inhibits motion along this reaction pathway.

The DET mechanism (reaction 4a) would be consistent with the most abundant product ions observed here of the type X^-. However, inspection of Figure 5 indicates that $\Delta H°_{4a}$ for most of the detectable reactions (several of which were fast) would be significantly endothermic. For example, the DET reaction $NB^- + CCl_4 \rightarrow NB + CCl_3 + Cl^-$, would be endothermic by 13 kcal mol^{-1}. Since the total thermal energy available in these two reactants at 125 °C is estimated to be no greater than about 7 kcal mol^{-1},[15] the DET mechanism, as it is written in reaction 4a, does not provide a satisfactory explanation for the moderately fast reaction observed here between NB^- and CCl_4.

The S_N2 displacement mechanism (reaction 5) would also be consistent with the ionic products observed here and might be thermodynamically feasible if a stable radical species of the type AR were formed along with X^-. However, in previous studies of gas-phase S_N2 reactions, CH_3I has been shown to be particularly susceptible to nucleophilic attack.[16] Therefore, the complete absence of reaction between CH_3I and any of the nucleophiles listed in Table I strongly suggests that this mechanism is not important for the reaction systems under investigation here. This result is not surprising in that the A^- anions used here are relatively large species with their excess charge delocalized over their extended π orbital system. Therefore, they do not possess a distinct atomic site at which nucleophilic attack and bond formation to the carbon center of the halomethanes are likely to occur.

CADET Mechanism. While the well-established mechanisms (reactions 4a, 4b, and 5) do not appear to adequately explain the reactions under investigation here, it will be shown here that they can be explained if a slight alteration of the DET mechanism is envisioned. This altered mechanism is illustrated in Figure 6 where the energetics associated with motion along the reaction coordinate are indicated for the specific case of A = NB and RX = CCl_4. The overall process consists of two distinct reactions. The first will be of principal importance in the discussions to follow and results in the overall transformation shown as reaction 8, in which

$$A^- + RX \rightarrow A{\cdot}X^- + R \qquad (8)$$

a clustered ion, $A{\cdot}X^-$, rather than a free halide ion, X^-, is produced along with the radical R. Due to the nature of this ionic product, reaction 8 will be called "cluster-assisted dissociative electron transfer" (CADET). The second reaction in Figure 6, also shown in reaction 9, is the well-known[11] declustering/clustering equilibria

$$A{\cdot}X^- \rightleftharpoons A + X^- \qquad (9)$$

reaction. Following reaction 8 and thermal equilibration of its product ion $A{\cdot}X^-$, the relative intensities of the $A{\cdot}X^-$ and X^- ions are subsequently held constant by reaction 9, which is fast in both directions. Due to a large positive entropy associated with reaction 9[11] and the relatively low concentration of the reagents, the higher energy products A + X^- are favored at 125 °C (for example, see above discussion of reaction 6 for the specific case of A = NB and X^- = Cl^-).

The nature of the potential surface proposed for the CADET mechanism in Figure 6 has precedence in Brauman's "double-well potential" model[13] for ion–molecule reactions that is now generally accepted and has been applied to many other reaction systems (including the slow electron-transfer reactions between SF_6 and molecular anions,[4] and between halomethanes and transition-metal complex negative ions[17]).

The CADET reaction (Figure 6) occurs by motion along a reaction coordinate on which special stability for two intermediate species is envisioned. The first intermediate $(A^-{\cdot}RX)^*$ is formed by an orbiting collision of the reagents with rate constant k_c. $(A^-{\cdot}RX)^*$ is assumed to be sufficiently long-lived for energy randomization to occur within it.[13] $(A^-{\cdot}RX)^*$ may back-decompose (k_b) or go over (k_p) the energy barrier that separates the two intermediates. The transition state at the height of the energy barrier is thought to resemble structure I (shown for the case of

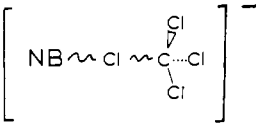

A = NB and RX = CCl_4) in which a C–Cl bond of CCl_4 is being ruptured as an electron is being transferred from NB^- to the Cl atom. The second intermediate $(A{\cdot}X^-{\cdot}R)^*$ consists of a halide ion, X^-, that is clustered by the molecule A and the radical R. If reaction 8 is exothermic, the fate of $(A{\cdot}X^-{\cdot}R)^*$ is decomposition to products $A{\cdot}X^-$ + R. The alternate decomposition pathway to products A + $X^-{\cdot}R$ is less likely due to the expected stronger clustering strengths of species A versus R.[11]

A steady-state kinetic treatment[4,13] of the system in Figure 6 provides the overall observed forward rate constant $k_f = k_c k_p/(k_p + k_b)$. A large structural change is expected to accompany the conversion of $(A^-{\cdot}RX)^*$ to $(A{\cdot}X^-{\cdot}R)^*$. If significant molecular motion is also required for the conversion of $(A^-{\cdot}RX)^*$ to the transition state, the energy barrier E_p can then exceed E_b so that $\Delta E^‡$ is positive (as shown in Figure 6). In that case, k_p will be smaller than k_b, and k_f will be smaller than the collision rate constant k_c.[13] As the potential energy of the reactants is increased by use of lower EA electron donors, the structure of the transition state is expected to shift toward that of $(A^-{\cdot}RX)^*$ (in accordance with the Hammond postulate and Marcus reaction rate theory.[18]). Along with this change, E_p would be lowered, k_p would be increased, and the observed rate constant would be increased until the limit $k_f = k_c$ is reached.

(15) Barrow, G. M. *Physical Chemistry*; McGraw-Hill: New York, 1973; p 109.
(16) Bierbaum, V. M.; Grabowski, J. J.; Depuy, C. H. *J. Phys. Chem.* **1984**, *88*, 1389.
(17) Jones, M. T.; McDonald, R. N.; Schell, P. L.; Ali, M. H. *J. Am. Chem. Soc.* **1989**, *111*, 5983.
(18) Lowry, T. H.; Richardson, K. S. *Mechanism and Theory in Organic Chemistry*; Harper and Row: New York, 1987; pp 212–229.

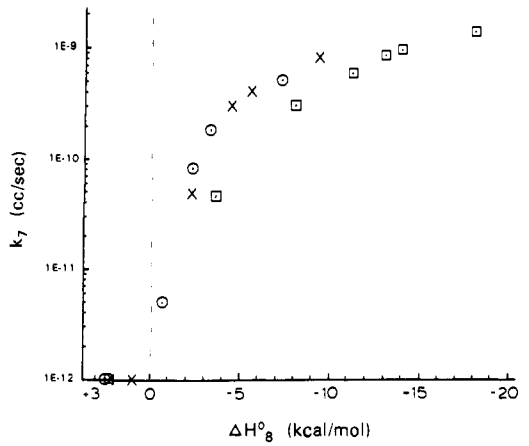

Figure 7. Observed second-order rate constants at 125 °C for the reactions of CCl_4 (○), CCl_3Br (×), and CF_2Br_2 (□) with molecular anions as a function of the enthalpy of reaction 8.

A central point of the CADET model is the proposition that the second intermediate species in Figure 6 is better represented as a complex ion of the type $(A{\cdot}X^-{\cdot}R)^*$ rather than as a pure electron transfer product, $(A{\cdot}RX^-)^*$. This provides a feasible explanation for the products observed in all of the reactions studied here since the most likely exit channel for $(A{\cdot}X^-{\cdot}R)^*$ is simple dissociation to $A{\cdot}X^-$ and R. This, along with the subsequent equilibrium reaction 9, accounts for the fact that ions of the type $A{\cdot}X^-$ and X^- are produced and ions of the type RX^- are not.

It will be shown in the remaining discussions that the wide range of reactivities observed for the eight halomethanes studied here can also be understood if viewed in terms of the CADET mechanism.

CCl_4, CCl_3Br, and CF_2Br_2. In Figure 7 the rate constants for the reactions of CCl_4, CCl_3Br, and CF_2Br_2 with the various molecular anions have been plotted against their calculated enthalpy for reaction 8. It is seen that the rate constants decrease precipitously as $-\Delta H°_8$ for each set of reactions approaches zero and are not detectable for any reactions systems having $-\Delta H°_8$ less than zero. This result is consistent with the proposition that the loss rate of A^- in the presence of CCl_4, CCl_3, or CF_2Br_2 is controlled by reaction 8.

As explained above, significant structural changes might be expected in the conversion of $(A^-{\cdot}RX)^*$ to the transition state for reaction systems of modest $-\Delta H°_8$. The reactions of NB^- and *m*-FNB^- with CCl_4 and of *o*-DNB^- with CCl_3Br are moderately exothermic, $\Delta H°_8 = -3.4$, -0.7, and -4 kcal mol^{-1}, respectively. Therefore, decreased reaction efficiencies (0.18, 0.005, and 0.05, respectively) and positive internal energy barrier heights ($\Delta E^{\ddagger}$ = +3.7, +6.8, and +2.5 kcal mol^{-1}, respectively) are observed for these three reactions (Table I). On the other hand, the CADET reaction of NB^- with CCl_3Br is significantly more exothermic ($\Delta H°_8 = -14$ kcal mol^{-1}, and this leads to unit reaction efficiency and no measurable activation barrier (Table I). In Figure 8, $\Delta E^{\ddagger}$ for the four reactions of CCl_4 and CCl_3Br have been plotted against the $\Delta H°_8$ of each reaction. The near coincidence of the two points B and C in Figure 8 suggests that the relationships between $\Delta E^{\ddagger}$ and $\Delta H°_8$ for the CCl_4 and CCl_3Br reaction systems are similar. It is interesting to note, however, that the rate constants for the CCl_4 reactions represented by point B are 3–4 times faster at all temperatures (Figure 4) than those represented by point C, even though $\Delta H°_8$ and $\Delta E^{\ddagger}$ for these two reactions are similar. This observation is consistent with a statistical advantage expected for the CADET reactions of CCl_4 versus those of CCl_3Br. That is, any one of four equivalent orientations of CCl_4 are possible in transition state I, while only one orientation of CCl_3Br in the transition state of its reactions leads to the product $A{\cdot}Br^-$.

$CFCl_3$ and CF_2Cl_2. $CFCl_3$ was found to undergo a detectable reaction only with the most energetic electron donor Az^- and CF_2Cl_2 was found to react with none of the electron donors. As

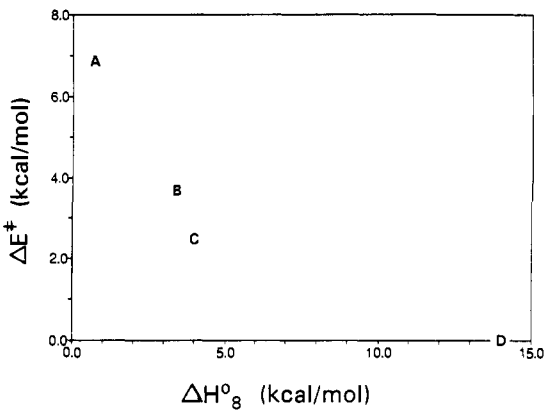

Figure 8. Activation energies determined from data in Figure 4 for the reactions of *m*-FNB^- with CCl_4 (A), NB^- with CCl_4 (B), *o*-NO_2NB^- with CCl_3Br (C), and NB^- with CCl_3Br (D).

shown in Figure 5, the energy of the products $A{\cdot}Cl^-$ + R involving $CFCl_3$ and CF_2Cl_2 are higher by about 1.5 and 4.0 kcal mol^{-1}, respectively, than the corresponding products of the CCl_4 reactions. This partially accounts for the slower reactions of $CFCl_3$ and CF_2Cl_2. Nevertheless, if the reactions of the two chlorofluoromethanes had followed the same trend as shown in Figure 7 for CCl_4, significantly greater rate constants might have been expected. For example, reaction 8 for Az^- with $CFCl_3$ is expected to be exothermic by 5.7 kcal mol^{-1}, but proceeds with a rate constant of only 2.3×10^{-11} cm^3 s^{-1}. Inspection of Figure 7 indicates that the rate constant for a CCl_4 reaction of similar exothermicity is expected to be about an order of magnitude greater. Also, while reaction 8 for Az^- with CF_2Cl_2 is expected to be exothermic by 3.2 kcal mol^{-1}, this reaction was not detectable. These results suggest that the CADET reactions of $CFCl_3$ and CF_2Cl_2 are being hindered by internal energy barriers that are higher than those of the CCl_4 reactions of similar $\Delta H°_8$.

A reasonable explanation for increased energy barriers in the CADET reactions of $CFCl_3$ and CF_2Cl_2 is provided by considering the major differences in the transition states for these systems relative to those involving CCl_4 (structure I). These differences are in the identity of the species R and its stabilizing influence of the transition state by virtue of its polarizability. In view of the known molecular polarizabilities, 11.2 Å^3 for CCl_4, 9.5 Å^3 for $CFCl_3$, 7.8 Å^3 for CF_2Cl_2, 5.6 Å^3 for CF_3Cl, and 3.8 Å^3 for CF_4,[19] a significant decrease in polarizability for R in the order $CCl_3 > CFCl_2 > CF_2Cl$ is expected. These decreases in the polarizability of R will tend to increase the height of the internal barrier, $\Delta E^{\ddagger}$, and decrease k_f in the CADET reactions of $CFCl_3$ and CF_2Cl_2 relative to those of CCl_4.

$CHCl_3$, CH_2Br_2, and CH_3I. For these three halohydromethanes, no reactions with NB^- were detectable and only weak reactivity was detected for $CHCl_3$ and CH_2Br_2 with Az^-. For $CHCl_3$, this result is expected since $\Delta H°_8$ is endothermic for all electron donors, except Az^-, for which $\Delta H°_8$ is approximately thermoneutral (Figure 5). In view of the energy level diagrams in Figure 5, however, the absolute nonreactivity of CH_3I and the marginal reactivity of CH_2Br_2 are extremely interesting. For example, $\Delta H°_8$ for the reactions of Az^- with CH_2Br_2 and with CH_3I are exothermic by about 7 and 11 kcal mol^{-1}, respectively. If these systems had followed the trends shown for CCl_4, CCl_3Br, and CF_2Br_2 in Figure 7, reaction efficiencies in excess of 0.5 might have been expected.

As in the cases of $CFCl_3$ and CF_2Cl_2 discussed above, the nonreactivity of CH_3I by the CADET mechanism can be at least partially attributed to the very low polarizability of the R species (CH_3) which would be involved in its transition state. Given that the polarizability of CH_4 is only 2.6 Å^3,[19] CH_3 would also be expected to have very low polarizability, leading to a relatively

(19) Weast, R. C.; Astle, M. J.; Beyer, W. H. *CRC Handbook of Chemistry and Physics*; CRC Press: Boca Raton, FL, 1988; p E-73.

large $\Delta E^{\ddagger}$. The large reduction in the reactivity of CH_2Br_2 relative to that of CF_2Br_2, however, cannot be convicingly attributed to polarizability effects. Since the polarizability of CH_2Br_2 (9.3 Å^3) is roughly the same[19] as that of CF_2Br_2 (9.0 Å^3), the species R = CH_2Br and CF_2Br might also be expected to have similar polarizabilities. Therefore, some additional factor appears to be responsible for the very low reactivity of CH_2Br_2 relative to that of CF_2Br_2.

The greater reactivity of CF_2Br_2 relative to that of CH_2Br_2 may reflect the importance of preferred orientations of these molecules in their ion complexes $(A^-\cdot RX)^*$ and their CADET transition states. CF_2Br_2 has a dipole moment of 0.66 D,[20] with the positive end located near the two bromine atoms. As the ion complex $(A^-\cdot CF_2Br_2)^*$ becomes tighter and moves toward its transition state, the ion-dipole force will tend to preferentially align the CF_2Br_2 molecule so that the bromine atoms point to the direction of A^-. A preference for this orientation with facilitate the forward conversion of $(A^-\cdot CF_2Br_2)^*$ to $(A\cdot Br^-\cdot CF_2Br)^*$. The dipole moment of CH_2Br_2 is larger (1.43 D) and has a polarity that is reversed relative to that of CF_2Br_2, so that its positive end is near its two hydrogen atoms. Therefore, the ion-dipole force in $(A^-\cdot CH_2Br_2)^*$ will tend to align the CH_2Br_2 molecule so that the bromine atoms point away from A^-. An increased preference for this orientation as $(A^-\cdot CH_2Br_2)^*$ moves toward its transition state will tend to inhibit its conversion to $(A\cdot Br^-\cdot CH_2Br)^*$. This factor would tend to lower the reactivity of CH_2Br_2 relative to that of CF_2Br_2, and would also lower the reactivities of $CHCl_3$ and CH_3I, since the dipole moments of these molecules (1.01 and 1.63 D, respectively) would also tend to align these molecules unfavorably within their CADET transition states.

(20) Weast, R. C.; Astle, M. J.; Beyer, W. H. *CRC Handbook of Chemistry and Physics*; CRC Press: Boca Raton, FL, 1988; p E-58.

Acknowledgment. This work was supported by the Chemical Analysis Division of the National Science Foundation under Grant CHE-9021330.

Symmetry-Breaking Solvent Effects on the Electronic Structure and Spectra of a Series of Triphenylmethane Dyes

Horst B. Lueck, Jeanne L. McHale,* and W. D. Edwards

Contribution from the Department of Chemistry, University of Idaho, Moscow, Idaho 83843.
Received August 26, 1991

Abstract: Solvent effects on the electronic structure of a series of para-substituted triphenylmethane dyes have been investigated using polarized Raman scattering and fluorescence spectroscopy, with interpretation aided by the results of intermediate neglect of differential overlap (INDO) molecular orbital calculations. While the evidence points to D_3 symmetry for the triphenylmethane cation in solution, resonance Raman and fluorescence data indicate that the symmetry of the substituted dyes is lowered by an interaction with the solvent. Semiempirical molecular orbital calculations support the idea that interaction of a charge or dipole with one of the amino groups could be responsible for breaking the symmetry of the crystal violet and parafuchsin ion, thus lifting the degeneracy of the excited electronic state which gives rise to absorption of visible light. The splitting of the excited electronic state shows up in the polarization dependence of both the resonance Raman spectra and the fluorescence emission. INDO calculations as well as fluorescence measurements argue against the existence of two ground-state conformations, such as a symmetric and an unsymmetric propeller form, as has been previously suggested.

Introduction

Para-substituted triphenylmethanes form a class of dyes for which there are a number of interesting structural questions concerning their solution-phase properties. In this work we examine the series shown in Figure 1: triphenylmethane (TPM), parafuchsin (PF), crystal violet (CV), ethylviolet (EV), malachite green (MG), and Victoria Pure Blue (VPB). One reason for interest in these compounds is the possible existence of twisted intramolecular charge-transfer (TICT) excited states,[1,2] for example, in CV. These have been investigated by a variety of time-resolved spectroscopic methods, such as two-photon fluorescence emission[3] and picosecond absorption spectroscopy.[4,5] Quantum mechanical calculations have been applied to the study of the torsional potential of TPM derivatives[1,6] and other molecules having TICT excited states.[7] Aggregation in solution, of certain of the dye derivatives (those with three amino groups), has been investigated spectroscopically.[8]

On the basis of X-ray crystallographic study of triphenylmethyl perchlorate,[9] and an older diffraction study of CV,[10] the expected geometry of the triply substituted dyes is a D_3 symmetric propeller form. Various investigations, however, have pointed to evidence that the symmetry of the solution-phase triply substituted dyes may be lower than D_3. For example, a magnetic circular dichroism (MCD) spectroscopic study suggested that TPM maintains its D_3 symmetry in solution, but that CV, although probably still in

(1) Vogel, M.; Rettig, W. *Ber. Bunsen-Ges. Phys. Chem.* **1985**, *89*, 962.
(2) Vogel, M.; Rettig, W. *Ber. Bunsen-Ges. Phys. Chem.* **1987**, *91*, 1241.
(3) Wirth, P.; Schnelder, S.; Dörr, F. *Opt. Commun.* **1977**, *20*, 155.
(4) (a) Menzel, R.; Hoganson, C. W.; Windsor, M. W. *Chem. Phys. Lett.* **1985**, *120*, 29. (b) Magde, D.; Windsor, M. W. *Chem. Phys. Lett.* **1974**, *24*, 144. (c) Cremers, D. A.; Windsor, M. W. *Chem. Phys. Lett.* **1980**, *71*, 27. (d) Sundström, V.; Gillbro, T.; Bergström, H. *Chem. Phys.* **1982**, *73*, 439. (e) Grzybowski, J. M.; Sugamori, S. E.; Williams, D. F.; Yip, R. W. *Chem. Phys. Lett.* **1979**, *65*, 456.
(5) (a) Ben-Amotz, D.; Harris, C. B. *Chem. Phys. Lett.* **1985**, *119*, 305. (b) Ben-Amotz, D.; Jeanloz, R.; Harris, C. B. *J. Chem. Phys.* **1987**, *86*, 6119.
(6) Dekkers, H. P. J. M.; Kielman-Van Luyt, E. C. M. *Mol. Phys.* **1976**, *31*, 1001.
(7) Majumdar, D.; Sen, R.; Bhattacharyya, K.; Battacharyya, S. P. *J. Phys. Chem.* **1991**, *95*, 4324.
(8) (a) Stork, W. H. J.; Lippitis, G. J. M.; Mandel, M. *J. Phys. Chem.* **1972**, *76*, 1772. (b) Sheppard, S. E.; Geddes, A. L. *J. Am. Chem. Soc.* **1944**, *66*, 1995. (c) Michaelis, L.; Granick, S. *J. Am. Chem. Soc.* **1945**, *67*, 1212.
(9) Gomes de Mesquita, A. H.; MacGillavry, C. H.; Eriks, K. *Acta Crystallogr.* **1965**, *18*, 437.
(10) Stora, C. *C. R. Acad. Sci., Ser. 2* **1958**, *246*, 1693.

0002-7863/92/1514-2342$03.00/0